UDC 678.742.3. 541.61. 544.163. *DOI: 10.15407/Surface.2024.16.130*

STRUCTURAL FEATURES AND MAGNETIC PROPERTIES OF IRON/POLYPROPYLENE COMPOSITES

Sevil Khalilova[1], Sevinj Osmanova[1,2], Aygun Rustamova[1], Lala Huseynova[3], Etibar Ismailov[1]

[1]Institute of Catalysis and Inorganic Chemistry, AZ1143, Baku Azerbaijan
[2] Khazar University, AZ1096, Baku Azerbaijan
[3]Azerbaijan State Oil and Industry University, AZ1010, Baku, Azerbaijan,
e-mail: sevilxalilova@gmail.com

Iron-containing polypropylene (PP) composites were synthesized by precipitating iron(III) nitrate from aqueous solutions of varying concentrations onto a polypropylene matrix, followed by drying at ≤110°C and heating at ≤230°C temperatures. The resulting composites were characterized using scanning electron microscopy combined with energy-dispersive elemental analysis (SEM/EDS), X-ray diffractometry (XRD), and electron magnetic resonance (EMR).The study revealed that the composites obtained through thermal decomposition of iron(III) nitrate from aqueous solutions on a polypropylene matrix, with subsequent heat treatment at 220°C, form a two-phase system consisting of isotactic polypropylene and magnetite. SEM/EDS data showed a non-uniform distribution of the iron-containing component on the PP surface, even in samples with less than 1% by weight of the iron component. FMR spectra indicated the formation of superparamagnetic and ferromagnetic particles within the polypropylene matrix, attributed to nanosized magnetite particles of varying dimensions.Theoretical spectra were calculated using the Landau-Lifshitz-Gilbert equation, considering Lorentzian, Gaussian, and Dyson resonance signal shapes. These theoretical spectra, which accounted for the dependence of g-factor values and line widths of the FMR spectra on particle size, were adjusted to match the experimental data to clarify the magnetic resonance characteristics of the iron-containing particles.The study concluded that magnetite particles formed during the thermal decomposition of iron(III) nitrate deposited from an aqueous solution onto the polypropylene matrix do not interact significantly with the polypropylene. These particles remain mobile on the polymer surface and are prone to aggregation, posing challenges for achieving a uniform composite material.

Keywords: *iron(III) nitrate, polypropylene, composites, thermal decomposition, SEM/EDS, XRD, EMR.*

INTRODUCTION

Over the past two decades, the interest of researchers in polymer-based composite materials containing nanosized metal, metal oxide particles has increased significantly due to the increased demands for them in various technological and industrial fields, in medicine etc.[1, 2]. Polypropylene (PP) stands out as an important general-purpose plastic due to its availability, non-toxicity, tastelessness and excellent mechanical properties. It is widely used in electrical appliances, automobiles and daily necessities [3, 4]. PP faces the problems of low impact strength and thermal stability. In order to expand the scope of PP, extensive research is focused on its modification in order to enhance its overall performance. The integration of various fillers, metal reinforcing elements, additives into the polymer matrix improves thermal, electrical and

mechanical properties [5 – 12]. The synergistic combination of fillers introduced into the polymer matrix offers a promising platform for the development of advanced functional materials with individual structural features, optical, electrical, magnetic, etc. properties. Magnetic properties of magnetite and polypropylene composites are of great interest, primarily from the point of view of biomedical applications [13, 14].

The list of methods for obtaining such composites is quite wide [15 – 20]. Structural features of metal oxide nanocomposites on polypropylene play a decisive role in determining their applicability. Understanding the morphology, phase composition and interfacial interactions in these composites is necessary to optimize their mechanical [21, 22], thermal and magnetic properties [23, 24]. Moreover, the magnetic properties of these composites depend on the size, shape and distribution of iron particles in the polypropylene matrix. Thus, detailed studies of the structural [25] and magnetic characteristics [26] of iron/iron oxide/polypropylene composites are necessary to advance their technological applications.

One of the simplest ways to obtain composite materials with a polypropylene base and iron, iron oxide filler is the thermal decomposition of salts deposited on a polymer matrix from aqueous solutions and organic solvents. The precipiated salts are subjected to thermal decomposition in various environments - oxidizing, reducing, neutral. Despite the huge number of works on the preparation of composite materials with a polypropylene base by thermal decomposition of iron salts, there is no information in the literature on the studies of thermal decomposition products with a polymer matrix, the mechanism of thermal decomposition of iron salts precipitated to a polypropylene matrix [27 – 29].

This paper presents the results of a study using SEM/EDS, X-ray diffraction and EMR of the structural features and magnetic properties of the thermal decomposition products of iron (III) nitrate precipitated to polypropylene from aqueous solutions.

MATERIALS AND METHODS

Materials. For obtaining iron-containing polymer composites based on polypropylene, the following were used as starting materials: pale mauve crystalline powder of iron nitrate $Fe(NO_3)_3$ x $9H_2O$ from CDH Central Drug House Ltd., isotactic polypropylene (PP) from the SOCAR Polymer plant with a melt flow rate of 23 g/10 min (at 230 ºC) and distilled water.

Synthesis of Fe/PP composites. Samples of iron-containing polymer composite based on polypropylene with different content of $Fe(NO_3)_3$ x $9H_2O$ (0.1, 1.0, 5.0, 10 and 15 wt. %) were obtained by precipitation of iron(III) nitrate to finely dispersed polypropylene powders at room temperature, followed by drying first at 110 °C for 4 hours and then heating at 220ºC in a muffle oven for 2 hours. In this way, samples of solid composite materials based on polypropylene Fe/PP with different iron content were obtained. For use in studies as a reference sample, the original polypropylene sample was also subjected to a similar procedure.

Charactesation techniques. The morphology, surface structure of the composite material, distribution of particles of the iron-containing component on its surface were studied using a scanning electron microscope coupled with an elemental analyzer (SEM/EDS, ThermoFisher Phenom Pro G6 with a BSD detector) at an accelerating voltage of 10 kV.

During the measurements, the cross sections of the samples were sputtered with a thin layer of gold for better resolution. The thickness of the taken Fe/PP samples submitted to the SEM/EDS analysis is around 0.5 mm.

Conclusions regarding the nature of the distribution of the iron-containing component on the surface of the polymer matrix were made on the basis of EDS analysis for iron content at 5 points arbitrarily selected on the surface of the polymer composite.

X-ray phase analysis of the obtained composite samples was carried out using a MiniFlex 300/600 device from Rigaku at a voltage of 40 kV and a current of 15 mA.

Ferromagnetic resonance (FMR) spectra of the samples were obtained using an EMXmicro spectrometer, Bruker in the temperature range of 77–500 K.

RESULT AND DISCUSSION

SEM/EDS Analysis. Fig. 1 and Fig. 2 show the SEM micrographs and EDS spectra of Fe/PP-1 (a) and Fe/PP-2 (b) composite samples, respectively, after drying at 110^{o}C for 4 hours and then heating at 220 ^{o}C for 2 hours (in current work, the synthesized 1 and 5 % Fe/PP composites were called as Fe/PP-1 and Fe/PP-2, accordingly).

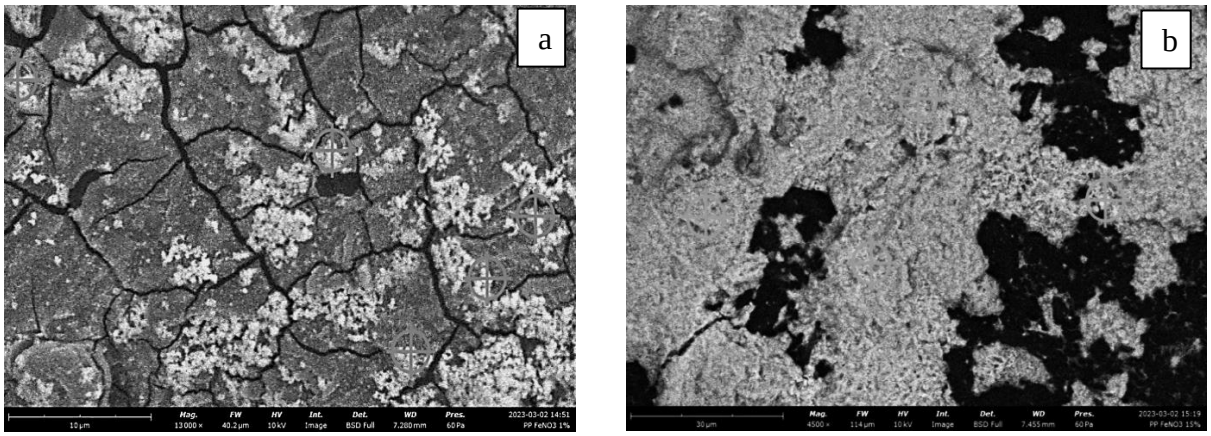

Fig. 1. SEM micrographs of Fe/PP-1 (a) and Fe/PP-2 (b) composites

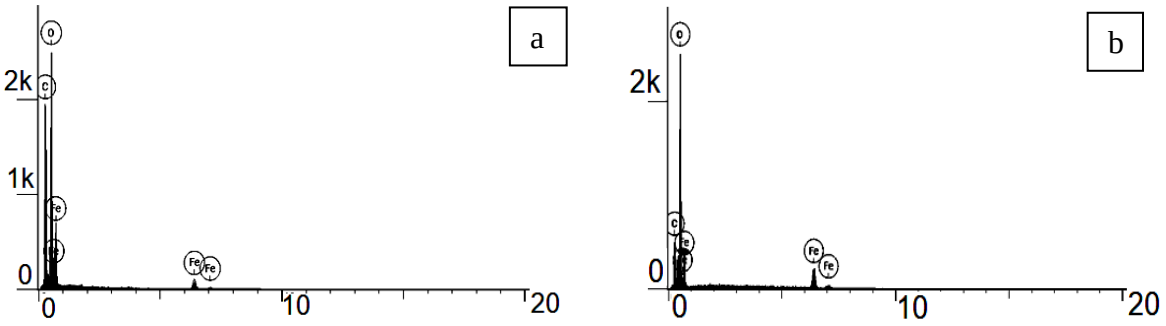

Fig. 2. EDS graphs of Fe/PP-1 (a) and Fe/PP-2 (b) composites

The results of determining the iron content at 5 points randomly selected on the surface of composites showed that even for composite samples containing only 0.5 wt% iron(III) nitrate after heat treatment, iron-containing particles are distributed non-uniformly. Table 1 shows the averaged values of carbon, oxygen and iron content for randomly selected samples on the surface of Fe/PP-1 and Fe/PP-2 composites.

Table 1. EDS data of Fe/PP-1 and Fe/PP-2 composites.

Element Number	**Element Symbol**	**Element contents in the composite, %**			
		Fe/PP-1		**Fe/PP-2**	
		Atomic	Weight	Atomic	Weight
6	C	47.556	26.600	10.299	4.600
8	O	33.952	25.300	61.342	36.500
26	Fe	18.492	48.100	28.358	58.900

According to the values of iron and oxygen content in the composites given in the Table 1, it can be concluded that the thermal decomposition of iron(III) nitrate precipitated to the polypropylene matrix is accompanied by the formation of iron oxides of at least two compositions, most likely Fe_3O_4 and Fe_2O_3. However, per below shown XRD analysis, only one phase, Fe_3O_4 magnetite, is recorded in the X-ray diffraction patterns.

XRD Analysis. Fig. 3 shows the X-ray patterns of iron nitrate crystal hydrate precipitated to polypropylene from an aqueous solution after drying at 110 °C for 4 hours and then heating at 220 °C for 2 hours.

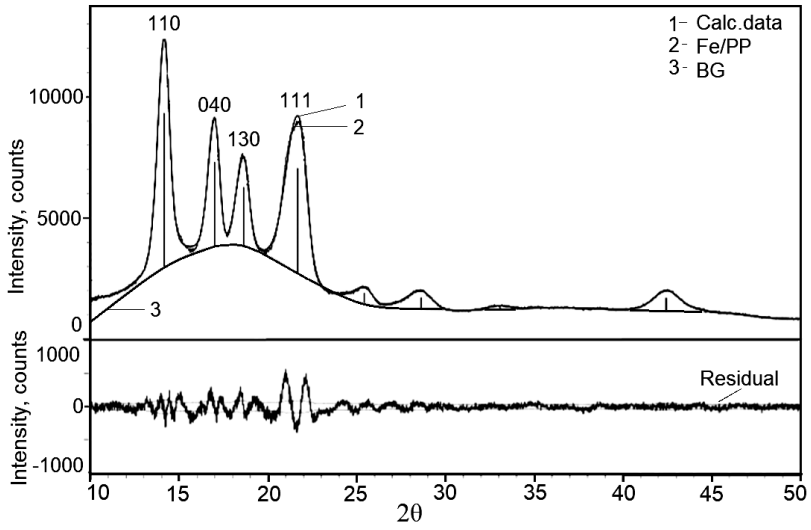

Fig. 3. The experimental and calculated (Rietveld) XRD patterns of Fe/PP-2 composite sample

The obtained X-ray diffraction patterns indicate the presence of only two phases in these samples, belonging to isotactic polypropylene and magnetite. Comparison of the X-ray diffraction patterns of pure PP and PP with iron-containing component shows that in the composite consisting of pure PP and the precipitated iron-containing component, there are no interactions leading to changes in the structure of the polymer and the iron-containing component. The obtained diffraction patterns do not show any changes in the crystal structure of the monoclinic α-form of PP. The diffraction patterns contain peaks at 2θ = 14, 16.9, 18.6 and 21.7°, corresponding to the crystal planes (110), (040), (130) and (111) of isotactic PP. The same peaks for PP are found in the diffraction patterns of the Fe/PP composite (Fig. 3). The diffractograms of the obtained composites also show peaks characteristic of magnetite. Tables 2–4 show the values of the structural parameters of magnetite and isotactic polypropylene, determined from the diffractograms obtained by the Rietfeld method.

Table 2. Lattice parameters of Fe-PP-2 composite

Phase name	a, Å	b, Å	c, Å	α, °	β, °	γ, °
Isotactic polypropylene	6.63901	20.80824	6.51284	90.000	99.500	90.000
Fe_3O_4	8.51307	8.51307	8.51307	90.000	90.000	90.000

Table 3 shows the angle, interval and intensity of the most intense diffraction lines of Fe_3O_4, which appear at 2θ = 18.03° (4.91 Å), 20.85° (4.25 Å), 29.65° (4.77 Å) and 3.00° (4.12 Å), etc. The interplanar distances (d), angle (2θ) and relative intensity of the most noticeable diffraction lines of PP belong to the crystalline monoclinic a-phase. The location coordinates of Fe and O atoms in the elementary lattice are given in Table 4.

Thus, it can be concluded that according to the diffraction patterns of the obtained composites consisting of an iron-containing component and polypropylene, no changes in the structure of the Fe/PP composites were detected.

Table 3. Interplanar spaces in Fe_3O_4

No.	2θ, °	d, Å	hkl	Norm. I.
1	18.03346	4.91502	111	100.00
2	20.85229	4.25654	200	49.29
3	29.65708	3.00982	220	37.80
4	34.92739	2.56679	311	45.38
5	36.53402	2.45751	222	23.99
6	42.43827	2.12827	400	29.12
7	46.45843	1.95303	331	16.44
8	47.73923	1.90358	420	17.11

Table 4. Structural parameters of Fe_3O_4 compound

Element	x	y	z	Occ.	B
Fe1(Fe)	0.500000	0.500000	0.500000	1.000	0.500
Fe2(Fe)	0.625300	0.625300	0.625300	1.000	0.500
O1(O)	0.381700	0.381700	0.381700	1.000	0.500
O2(O)	0.872200	0.872200	0.872200	1.000	0.500
Fe3(Fe)	0.000000	0.000000	0.000000	1.000	0.500

FMR analysis. Fig. 4 shows the experimental FMR spectra of iron (III) nitrate crystal hydrate precipitated to the polypropylene from an aqueous solution with different concentrations after drying at 110°C.

The FMR spectra shown in Fig. 4 belong to synthesized Fe-PP composite samples containing 1 and 5 % iron content, accordingly. As can be seen from Fig. 4, asymmetric signals are observed in the FMR spectra of these samples, which most likely belong to nanosized iron-containing particles of different sizes. Table 5 shows the values of the line width ΔH, the position of the resonance field H_{res} and the relative integral intensities $I_{int} = A*(\Delta H)^2$ (A is the signal amplitude) of the samples.

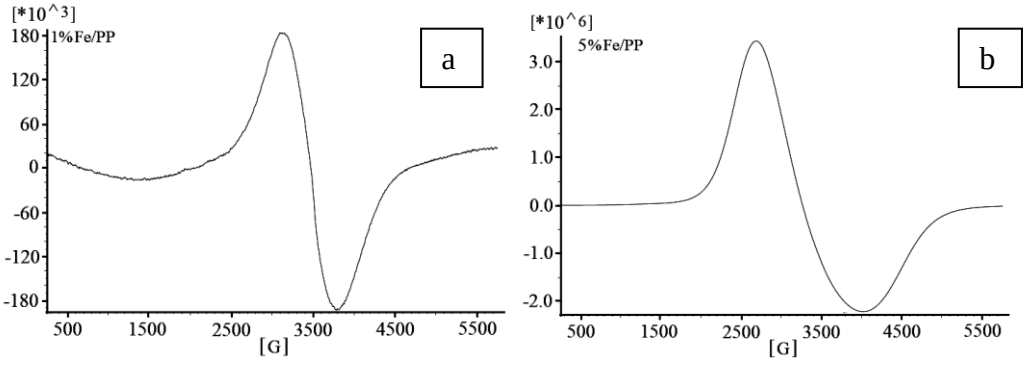

Fig. 4. The FMR spectra of Fe/PP-1 (a) and Fe/PP-2 (b) composites

Table 5. The values of FMR parameters of Fe/PP-1 and Fe/PP-2 composites

Sample	Resonance field, H_{res}, mT	Line width, ΔH, mT	Intensity, I_{int}, a.u.,	g_{eff}
Fe/PP-1	345	73	1.0	2.04
Fe/PP-2	330	130	13.9	2.13

As can be seen from Table 5, with increasing concentration of the iron-containing component, the resonance line shifts to the region of weaker magnetic fields, and its width and intensity increase. For Fe_3O_4 nanoparticles ~2.5 nm in size embedded in polyethylene, the FMR method recorded a line with a line width of ΔH = 40 mT with a center of g ~ 2.07 [30, 31]. Modeling of the FMR spectra of iron oxide showed that the intensity and width of the line increase significantly with increasing nanoparticle size. For 10 nm nanoparticles, the FMR spectrum is almost the same as that obtained in [32]

Theoretical analysis shows that the spectra shown in Fig. 5 (a, b) consist of at least two signals with different values of g-factors, intensities and line widths. It is assumed that, both signals, namely with the g-factor values equal to 2.04 and 2.13, line widths of 73 mT and 130 mT, according to the XRD results, belong to nanosized magnetite particles, but with different sizes. Fig. 6 shows the FMR spectra calculated based on the Landau-Lifshitz and Gilbert equations for particles with average sizes of 8 – 10 and 15 – 20 nm in the particle size distribution range of 2 – 100 and using Monte Carlo calculation. The studies have shown that the calculated spectrum is well adjusted to the experimental one when these spectra are superimposed at a ratio of 2:5.

Fig. 5 shows the FMR spectra calculated on the basis of the Landau-Lifshitz-Gilbert equation under the assumption of a Lorentzian shape of the FMR curve by fitting the theoretically calculated spectrum to the experimental one. This showed the best convergence of the theoretically created spectrum with the experimental one for magnetite particles with an average size of 10 nm and below.

The fitting of the theoretically calculated spectrum to the experimental one showed the best convergence of the theoretically created with the experimental one for magnetite particles with average sizes of 8–10 and 15–20 nm with a combination of theoretically calculated spectra for these sizes in a ratio of 2:5.

Magnetite (Fe_3O_4) is a ferrimagnet. The ferrimagnetism of magnetite is due to its structure. Magnetite has an inverse spinel structure, where oxygen ions form a cubic close packing, and iron cations occupy octahedral and tetrahedral positions: Fe^{3+} and Fe^{2+} ions are in octahedral positions and only Fe^{3+} ions are in tetrahedral positions. In magnetite, the interaction between iron ions occurs through exchange interaction, which depends on their position in the crystal lattice. The manifestation of ferrimagnetic properties in magnetite is due to the fact that the total magnetic moment of octahedral ions exceeds the total magnetic moment of tetrahedral ions. This leads to the presence of a residual magnetic moment, which determines the ferrimagnetism of the material.

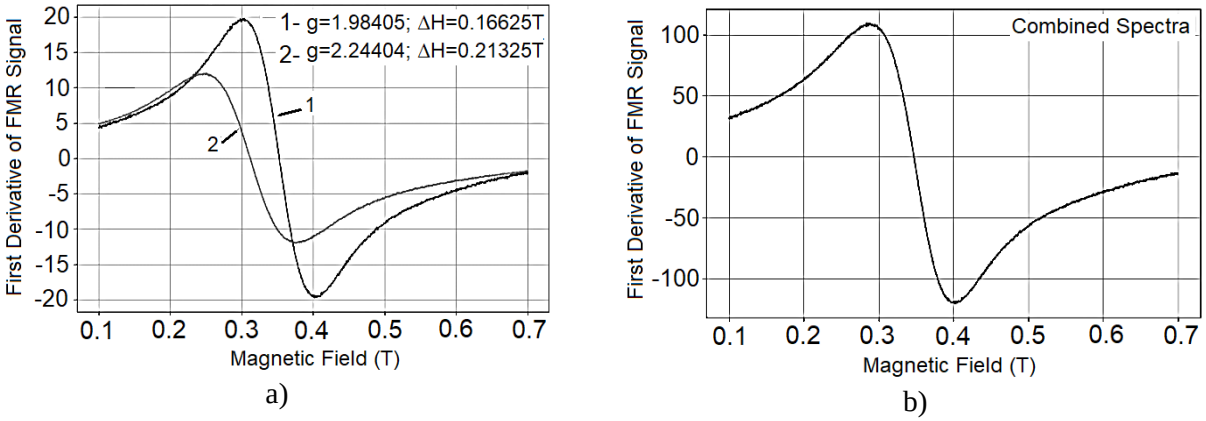

Fig.5. FMR spectra calculated on the basis of the Landau-Lifshitz-Gilbert equation under the assumption of the Lorentzian shape of the FMR curve

Ferrimagnet Fe_3O_4 becomes paramagnet at temperatures above 858 K. This is for a massive sample. The temperature of the transition from the ferrimagnetic state to the paramagnetic depends on the size of the particles. Fig. 6 shows the transition temperature of ferrimagnet to paramagnet for a bulk Fe_3O_4 sample and the dependence of this temperature from the particle size of magnetite in the range of 1–100 nm.

For convenience, a horizontal line has been added indicating room temperature (300 K) in order to show at what particle sizes magnetite remains ferrimagnetic at room temperature. In [33], lowering the Curie temperature for nanoparticles is discussed and experimental data and models were given for various materials, including Fe_3O_4.

As can be seen from Fig.6(b), magnetite samples with particle sizes less than 15 nm are superpara/paramagnetic at room temperature and below.

Fig. 7 shows a histogram of the distribution of the sizes of Fe_3O_4 particles with a mode of 8 nm, calculated under the assumption of their lognormal distribution. The histogram shows the frequency of different particle sizes in nanometers. Fig. 8 shows the FMR spectra calculated for Fe_3O_4 particles of different sizes (5, 10, 20, 50 nm). These spectra show how the shape and intensity of the spectra change depending particle size.

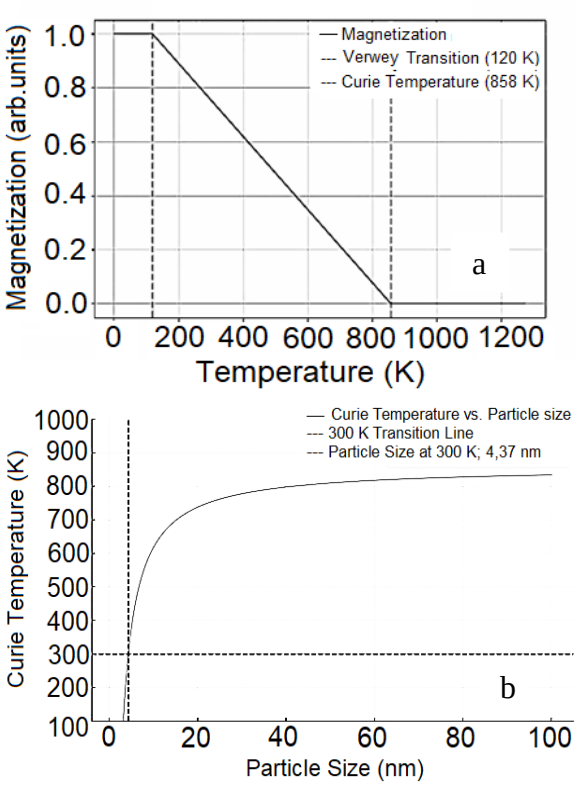

Fig. 6. The transition temperature of ferrimagnetic-paramagnetic:
a) for a bulk Fe_3O_4 sample
b) the dependence from the particle size of magnetite in the range of 1–100 nm

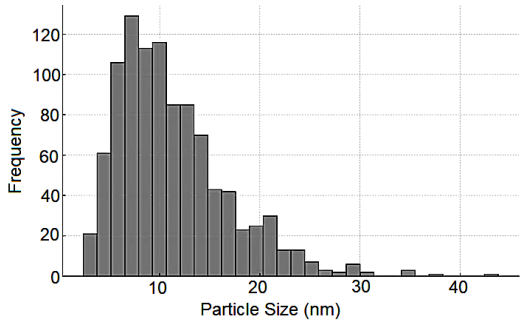

Fig. 7. Histogram of the distribution of Fe_3O_4 particle sizes calculated under the assumption of a lognormal distribution

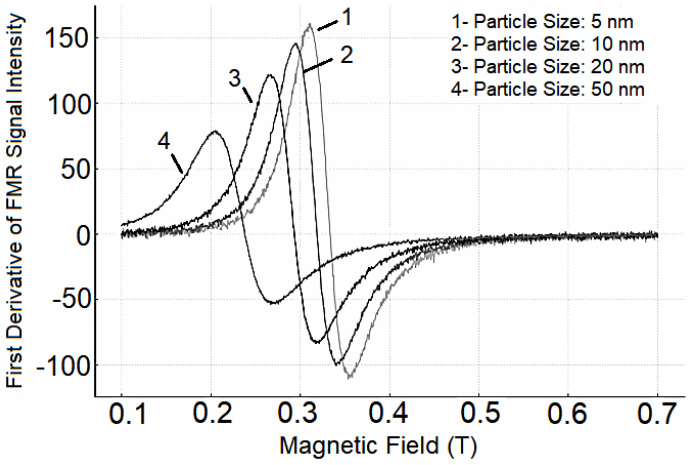

Fig. 8. FMR spectra calculated for Fe_3O_4 particles of different sizes (5, 10, 20, 50 nm)

As can be seen from Fig. 8, the FMR spectra differ in line width and resonance field position, which is due to changes in the g-factor and line width depending on the particle size. The graph clearly shows how the shape and intensity of the spectra change for Fe_3O_4 particles of different sizes (5, 10, 20, 50 nm) and how the FMR spectra can be used to estimate the size of nanoparticles in a sample.

CONCLUSION

For polymer-based composites, especially those with a polyethylene, polypropylene, or similar base, the primary challenge is achieving homogeneous distribution of "metallic" and metal-oxide components. This study demonstrates that it is impossible to obtain a composite with homogeneously distributed magnetite particles through the thermal decomposition of an aqueous solution of iron(III) nitrate precipitated onto a polypropylene matrix. No information was found on studies addressing the distribution of metal or metal-oxide components in composites with a polypropylene, polyethylene, or similar base, nor on the synthesis of such composites via thermal decomposition of various metal salts precipitated from different solutions to achieve a uniform distribution of metal and/or metal-oxide components within the polymer matrix. We believe the main issue lies in the nature of the polymer matrix. Polypropylene and similar hydrocarbon matrices are inert, causing the metal and/or metal-oxide particles formed during the thermal decomposition of salts to remain unbound to the polymer matrix. These particles are highly mobile on the polymer surface, leading to easy aggregation.

REFERENCES

1. Osman A.F., Mariatti M. Properties of Aluminum Filled Polypropylene Composites. *Polym. Polym. Compos*. 2006. 14(6): 623.
2. Taşdemır M., Gülsoy H.Ö. Mechanical Properties of Polymers Filled with Iron Powder. *Int. J. Polym. Mater*. 2008. 57(3): 258.
3. Altan M., Yildirim H., Uysal A. Tensile properties of polypropylene/metal oxide nano composites. *TOJST*. 2011. 1(1): 25.
4. Moravskyi V., Kucherenko A., Kuznetsova M., Dulebova L., Spišák E., Majerníková J. Utilization of Polypropylene in the Production of Metal-Filled Polymer Composites: Development and Characteristics. *Materials*. 2020. 13(12): 2856.

5. Dabees S., Elshalakany A., Tirth V., Kamel B.M. Synthesis and characterization studies of high-density polyethylene-based nanocomposites with enhanced surface energy, tribological, and electrical properties. *Polymer Testing*. 2021. 98: 107193.
6. Wu Y., Xu L., Jiang Y. Preparation and Thermal Properties of Modified Cu_2O/ Polypropylene (PP), *Compos. Mater*. 2020. 13: 309.
7. Yurkov Yu., Kozinkin A.V., Nedoseikina T.I., Shuvaev A.T. et al. Copper Nanoparticles in a Polyethylene Matrix. *Inorg. Mater*. 2001. 37(10): 997.
8. Ong H.L., Akil H.M, Mahmud Sh. Effect of Particle Morphology on the Properties of Polypropylene/Nanometric Zinc Oxide (PP/Nanozno) Composites. *Adv. Compos. Lett.* 2009. 18(3): 77.
9. Silva C., Bobillier F., Canales D., Sepúlveda F.A., etc. Mechanical and Antimicrobial Polyethylene Composites with CaO Nanoparticles. *Polymers.* 2020. 12(9): 2132.
10. Gupta N., Paramsothy M. Metal- and Polymer-Matrix Composites: Functional Lightweight Materials for High-Performance Structures. *JOM.* 2014. 66(6): 862.
11. Griffiths E., Wilmers J., Bargmann S., Reddy B.D. Nanoporous metal based composites: Giving polymers strength and making metals move. *J. Mech. Phys. Solids.* 2020. 137: 103848.
12. Kalia S., Kango S., Kumar A., Haldorai Y. Magnetic polymer nanocomposites for environmental and biomedical applications. *Colloid Polym Sci.* 2014. 292: 2025.
13. Karna S.K., Mishra S.R., Gunapala E., Dubenko I. et al. Synthesis and Characterization of FeNi /Polymer Nanocomposites. *JNN*. 2010. 10(9): 5879.
14. .Nisar M., Bernd M., Filho L., Geshev J. Polypropylene/carbon nanotube magnetic composites obtained using carbon nanotubes from sawdust. *Polym. Advan. Technol.* 2019. 30(2): 457.
15. He Q., Yuan T., Zhu J., Luo Z., et al. Magnetic high density polyethylene nanocomposites reinforced with in-situ synthesized Fe@FeO core-shell nanoparticles. *Polymer*. 2012. 53: 3642.
16. Wang Y., Li J., Zhang Z., Wang J., et al. Magnetic polypropylene composites with selectively localized reactive nano-Fe_3O_4 in toughener of POE-g-MAH: Towards super toughness, high flexibility and balanced strength. *Mater. Des*. 2022. 217: 110607.
17. Carosio F., Fina A., Coisson M. Polypropylene-based ferromagnetic composites. *Polymer Bulletin*. 2010. 65(7): 681.
18. Shirinova H., Palma L.D., Sarasini F., Tirillò J. Synthesis and Characterization of Magnetic Nanocomposites for Environmental Remediation. *Chem. Eng. Trans*. 2016. 47: 103.
19. Orellana F., Lisperguer J., Nuñez C. Synthesis and characterization of polypropylene-silica, alumina and titania nanoparticles, prepared by melting. *J. Chil. Chem. Soc.* 2014. 59(1): 2389.
20. Reinholds I., Kalkis V., Zicans J., Meri R.M. Mechanical, structural and magnetic properties of polypropylene/iron ferrite magnetic nanocomposites. *IOP Conf. Series: Materials Science and Engineering*. 2012. 38: 012030.
21. Palma L.D., Bavasso I., Sarasini F., Tirillo J. Effect of nano-magnetite particle content on mechanical, thermal and magnetic properties of polypropylene composites. *Polym. Compos.* 2018. 39: E1742.
22. Koo J., Kim H., Kim K, Jang Y.R., et al. Controlling the magnetic properties of polymer–iron oxide nanoparticle composite thin films via spatial particle orientation. *RSC Adv.* 2016. 6: 55842.
23. Novakova A.A., Lanchinskaya V.Yu., Volkov A.V., Gendler T.S. Magnetic properties of polymer nanocomposites containing iron oxide nanoparticles. *J. Magn. Magn. Mater.* 2003. 258–259: 354.

24. Taha T.A.M., Tharwat M., Ismael A. A Comprehensive Study of Structural, Thermal, and Dielectric Properties of Melt-Processed Polypropylene/$Ni_{0.9}Zn_{0.1}Fe_2O_4$ Nanocomposites. *J. Compos. Sc*i. 2024, 8(4): 117.
25. Mandiola B.C., Bolados H.A., Geshev J., Quíjada R. Study of the Influence of Magnetite Nanoparticles Supported on Thermally Reduced Graphene Oxide as Filler on the Mechanical and Magnetic Properties of Polypropylene and Polylactic Acid Nanocomposites. *Polymers (Basel).* 2021. 13(10): 1635.
26. Bui T.Q., Ton S.N., Duong A.T., Tran H.T. Size-dependent magnetic responsiveness of magnetite nanoparticles synthesised by co-precipitation and solvothermal methods. *J. Sci.: Adv. Mater. Devices*. 2018. 3: 107.
27. Khalilova S.R., Osmanova S.N., Ismailov E.H. Synthesis of iron-polypropylene and iron-high density polyethylene composites. *Chem. Sci. Symp. 2023: Chemistry of polymers. Books of abstacts.* (October 26–27, 2023, London, UK). P. 079.
28. Khalilova S.R., Rustamova A.I., Osmanova S.N., Ismailov E.H. Synthesis and Characterization of Iron-containing PP and HDPE based composites. *2nd Int. Sci Conf., Book of abstacts*, (November 23–25, 2023, Tbilisi, Georgia). P. 22.
29. Zapata P., Quijada R. Polypropylene Nanocomposites Obtained by In Situ Polymerization Using Metallocene Catalyst: Influence of the Nanoparticles on the Final Polymer Morphology. *J. Nanomater*. 2012. 1: 194543.
30. Gubin S.P., Spichkin Y.I, Yurkov G.Yu., Tishin A.M. Nanomaterial for High-Density Magnetic Data Storage. *Russ. J. Inorg. Chem*. 2002. 47(1): S32.
31. Guskos N., Typek J., Maryniak M., Roslaniec Z.,Petridis D.,Kwiatkowska. M. FMR study of γ-Fe_2O_3 magnetic nanoparticles in a multiblock poly(ether-ester) copolymer matrix. *Materials Science-Poland.* 2005. 23(4): 57.
32. Guskos N., Maryniak M., Typek J, Pełech I. et al. Temperature Dependence of the FMR Spectra of Polymer Composites with Nanocrystalline α-Fe/C filler. *SSP*. 2007. 128: 213.
33. Broek J., et al. Size effect on the Curie temperature of ferromagnetic nanoparticles. *J. Magn. Magn. Mater*. 2010. **322**(3).

УДК 678.742.3. 541,61. 544.163. *DOI: 10.15407/Surface.2024.16.130*

СТРУКТУРНІ ОСОБЛИВОСТІ ТА МАГНІТНІ ВЛАСТИВОСТІ КОМПОЗИТІВ ЗАЛІЗО/ПОЛІПРОПІЛЕН

Севіль Халілова[1], Севіндж Османова[1,2], Айгюн Рустамова[1], Лала Гусейнова[3], Етібар Ісмаїлов[1]

[1]Інститут каталізу та неорганічної хімії, AZ1143, Баку, Азербайджан
[2]Хазарський університет, AZ1096, Баку, Азербайджан
[3]Азербайджанський державний університет нафти та промисловості, AZ1010, Баку, Азербайджан, е-пошта: sevilxalilova@gmail.com

Залізовмісні поліпропіленові (ПП) композити синтезували осадженням нітрату заліза(III) з водних розчинів різної концентрації на поліпропіленову матрицю з наступним висушуванням при ≤110 °C і нагріванням при ≤230°C. Отримані композити охарактеризовані методами скануючої електронної мікроскопії в поєднанні з енергодисперсійним елементним аналізом (SEM/EDS), рентгенівською дифрактометрією (XRD) та електронно-магнітним резонансом (EMR). Дослідження показало, що композити, отримані термічним розкладанням заліза (III) нітрати з водних розчинів на поліпропіленовій матриці з подальшою термічною обробкою при 220 °C утворюють

двофазну систему ізотактичного поліпропілену та магнетиту. Дані SEM/EDS показали нерівномірний розподіл залізовмісного компонента на поверхні поліпропілену навіть у зразках із вмістом заліза менше ніж 1% за вагою. Спектри ЕМР вказують на утворення суперпарамагнітних і феромагнітних частинок у поліпропіленовій матриці, які зв'язані з нанорозмірними частинками магнетиту різних розмірів. Теоретичні спектри розраховувалися за рівнянням Ландау-Ліфшица-Гільберта з урахуванням форм резонансного сигналу Лоренца, Гауса та Дайсона. Ці теоретичні спектри, які враховували залежність значень g-фактора та ширини ліній спектрів ЕМР від розміру частинок, були скориговані відповідно до експериментальних даних для уточнення характеристик магнітного резонансу залізовмісних частинок. Дослідження показало, що частинки магнетиту, що утворюються при термічному розкладанні нітрату заліза(III), нанесеного з водного розчину на поліпропіленову матрицю, суттєво не взаємодіють з поліпропіленом. Вони залишаються рухливими на поверхні полімеру та схильні до агрегації, що створює проблеми для досягнення однорідного композитного матеріалу.

Ключові слова: *нітрат заліза(III), поліпропілен, композити, термічний розклад, SEM/EDS, XRD, EMR.*

APPENDIX

Below is the Python code for calculating FMR spectra, their first derivatives for Fe_3O_4 nanoparticles at different temperatures using the Dyson line shape, taking into account the temperature dependences of the g-factor and line width. The spectra can be presented either separately for each temperature or together for comparison (Fig. 5).

```
python
import numpy as np
import matplotlib.pyplot as plt

# Constants
mu_B = 9.274009994e-24  # Bohr magneton in J/T
h = 6.62607015e-34  # Planck's constant in J*s
frequency = 9.8e9  # Hz
gamma = 2 * np.pi * frequency / mu_B  # gyromagnetic ratio
# Base parameters
T_0 = 300  # Reference temperature in K
g_0 = 2.1  # Base g-factor, approximate value
k_g = -1.5e-4  # K^-1, temperature coefficient for g-factor
Delta_H_0 = 0.1  # Tesla, base linewidth
k_Delta_H = 2.5e-4  # Tesla/K, temperature coefficient for linewidth

# Magnetic field range
H = np.linspace(0.1, 0.7, 1000)  # Tesla

# Dyson line shape function
def dyson_line_shape(H, H_res, delta_H, asymmetry):
    lorentz = (delta_H / (2 * np.pi)) / ((H - H_res) ** 2 + (delta_H / 2) ** 2)
    dispersive = (H - H_res) / ((H - H_res) ** 2 + (delta_H / 2) ** 2)
    return (1 - asymmetry) * lorentz + asymmetry * dispersive

# Function to compute the first derivative of Dyson line shape
def dyson_line_shape_derivative(H, H_res, delta_H, asymmetry):
    dyson = dyson_line_shape(H, H_res, delta_H, asymmetry)
    return np.gradient(dyson, H)

# Temperatures to analyze
temperatures = [77, 300, 473, 673]
```

```
# Calculate and plot FMR spectra and their first derivatives
plt.figure(figsize=(12, 8))
for T in temperatures:
    g_factor = g_0 + k_g * (T - T_0)
    Delta_H = Delta_H_0 + k_Delta_H * (T - T_0)

    H_res = frequency * h / (g_factor * mu_B)

    asymmetry = 0.1  # Example value for asymmetry parameter in Dyson line shape
    spectrum = dyson_line_shape(H, H_res, Delta_H, asymmetry)
    spectrum_derivative = dyson_line_shape_derivative(H, H_res, Delta_H, asymmetry)

    # Plot FMR spectrum
    plt.plot(H, spectrum, label=f'Temperature: {T}K - Spectrum')

    # Plot first derivative of FMR spectrum
    plt.plot(H, spectrum_derivative, label=f'Temperature: {T}K - First Derivative')

# Plot settings
plt.title('FMR Spectra and Their First Derivatives for Fe3O4 Nanoparticles with Dyson Line Shape')
plt.xlabel('Magnetic Field (T)')
plt.ylabel('Intensity')
plt.legend()
plt.grid(True)
plt.show()

# Plot FMR spectra and their first derivatives separately
for T in temperatures:
    g_factor = g_0 + k_g * (T - T_0)
    Delta_H = Delta_H_0 + k_Delta_H * (T - T_0)

    H_res = frequency * h / (g_factor * mu_B)

    asymmetry = 0.1  # Example value for asymmetry parameter in Dyson line shape
    spectrum = dyson_line_shape(H, H_res, Delta_H, asymmetry)
    spectrum_derivative = dyson_line_shape_derivative(H, H_res, Delta_H, asymmetry)

    # Plot FMR spectrum
    plt.figure(figsize=(12, 8))
    plt.plot(H, spectrum, label='FMR Spectrum')
    plt.title(f'FMR Spectrum for Fe3O4 Nanoparticles at {T}K')
    plt.xlabel('Magnetic Field (T)')
    plt.ylabel('Intensity')
    plt.legend()
    plt.grid(True)
    plt.show()

    # Plot first derivative of FMR spectrum
    plt.figure(figsize=(12, 8))
    plt.plot(H, spectrum_derivative, label='First Derivative of FMR Spectrum')
    plt.title(f'First Derivative of FMR Spectrum for Fe3O4 Nanoparticles at {T}K')
    plt.xlabel('Magnetic Field (T)')
    plt.ylabel('Intensity')
    plt.legend()
    plt.grid(True)
    plt.show()
```